Mechanism of Ene Reactions of Singlet Oxygen. A Two-Step No-Intermediate Mechanism

Daniel A. Singleton,*,[†] Chao Hang,[†] Michael J. Szymanski,[†] Matthew P. Meyer,[†] Andrew G. Leach,[‡] Keith T. Kuwata,[§] Jenny S. Chen,[‡] Alexander Greer,[‡] Christopher S. Foote,*,[‡] and K. N. Houk*,[‡]

Contribution from the Department of Chemistry, Texas A&M University, P.O. Box 30012, College Station, Texas 77842, Department of Chemistry and Biochemistry, University of California, Los Angeles, California 90095-1569, and Department of Chemistry, Macalester College, Saint Paul, Minnesota 55105-1899

Received June 7, 2002; E-mail: singleton@mail.chem.tamu.edu

Abstract: The mechanism of the ene reaction of singlet ($^1\Delta_g$) oxygen with simple alkenes is investigated by a combination of experimental isotope effects and several levels of theoretical calculations. For the reaction of 2,4-dimethyl-3-isopropyl-2-pentene, the olefinic carbons exhibit small and nearly equal ^{13}C isotope effects of 1.005−1.007, while the reacting methyl groups exhibit ^{13}C isotope effects near unity. In a novel experiment, the ^{13}C composition of the product is analyzed to determine the intramolecular ^{13}C isotope effects in the ene reaction of tetramethylethylene. The new ^{13}C and literature ^{2}H isotope effects are then used to evaluate the accuracy of theoretical calculations. RHF, CASSCF(10e, 8o), and restricted and unrestricted B3LYP calculations are each applied to the ene reaction with tetramethylethylene. Each predicts a different mechanism, but none leads to reasonable predictions of the experimental isotope effects. It is concluded that none of these calculations accurately describe the reaction. A more successful approach was to use high-level, up to CCSD(T), single-point energy calculations on a grid of B3LYP geometries. The resulting energy surface is supported by its accurate predictions of the intermolecular ^{13}C and ^{2}H isotope effects and a very good prediction of the reaction barrier. This CCSD(T)//B3LYP surface features two adjacent transition states without an intervening intermediate. This is the first experimentally supported example of such a surface and the first example of a valley−ridge inflection with significant chemical consequences.

Introduction

For a continuous function of a single variable, there must be a minimum between any two maxima. When this idea is applied to reaction coordinate diagrams drawn on paper, it might be concluded that there must be an intermediate between two transition states (Figure 1a). Indeed, this idea lies behind rules for the interpretation of mechanistic data as evidence for intermediates. In higher dimensions, however, a transition state is a saddle point, not a maximum, and an energy surface can readily have two adjacent saddle points with no intervening minimum (Figure 1b).[1] On such surfaces, the reaction path bifurcates, and a selection between possible products occurs after the initial transition state. This selection occurs in an area of the surface referred to as the *valley−ridge inflection*.[1−5] Theoretical studies have predicted surfaces of this type for a number of simple reactions, including the ring opening of cyclopropylidene to form allene,[2] pseudorotations in SiH_4F^- and PH_4F,[3] 1,2-hydrogen migration in $H_3CO^\bullet$,[4] the photodissociation of thioformaldehyde,[5] reactions of ketyl anion radicals with methyl halides,[6] and bond shifting in cyclooctatetraene.[7] Recent theoretical calculations by Caramella and co-workers have intriguingly predicted a symmetrical bifurcating surface for the Diels−Alder dimerization of cyclopentadiene.[8] Whenever symmetry is broken after an initial symmetrical transition state, the reaction path must bifurcate. This makes numerous other reactions, such as the dimerizations of cyclobutadiene and cyclopropene,[9] strong candidates for the type of surface in Figure 1b.

---

† Texas A&M University.
‡ University of California.
§ Macalester College.

(1) Metiu, H.; Ross, J.; Silbey, R.; George, T. F. *J. Chem. Phys.* **1974**, *61*, 3200.
(2) Valtazanos, P.; Ruedenberg, K. *Theor. Chim. Acta* **1986**, *69*, 281. Valtazanos, P.; Elbert, S. T.; Ruedenberg, K. *J. Am. Chem. Soc.* **1986**, *108*, 3147.
(3) Windus, T. L.; Gordon, M. S.; Burggraf, L. W.; Davis, L. P. *J. Am. Chem. Soc.* **1991**, *113*, 4356. Windus, T. L.; Gordon, M. S. *Theor. Chim. Acta* **1992**, *83*, 21.

(4) (a) Yanai, T.; Taketsugu, T.; Hirao, K. *J. Chem. Phys.* **1997**, *107*, 1137. (b) Kumeda, Y.; Taketsugu, T. *J. Chem. Phys.* **2000**, *113*, 477. (c) Taketsugu, T.; Kumeda, Y. *J. Chem. Phys.* **2001**, *114*, 6973.
(5) Tachibana, A.; Okazaki, I.; Koizumi, M.; Hori, K.; Yamabe, T. *J. Am. Chem. Soc.* **1985**, *107*, 1190.
(6) (a) Bakken, V.; Danovich, D.; Shaik, S.; Schlegel, H. B. *J. Am. Chem. Soc.* **2001**, *123*, 130. (b) Yamataka, H.; Aida, M.; Dupuis, M. *Chem. Phys. Lett.* **1999**, *300*, 583.
(7) Castaño, O.; Palmeiro, R.; Frutos, L. M.; Luisandrés, J. *J. Comput. Chem.* **2002**, *23*, 732. See also Wenthold, P. G.; Hrovat, D. A.; Borden, W. T.; Lineberger, W. C. *Science* **1996**, *272*, 1456. Hrovat, D. A.; Borden, W. T. *J. Am. Chem. Soc.* **1992**, *114*, 5879.
(8) Caramella, P.; Quadrelli, P.; Toma, L. *J. Am. Chem. Soc.* **2002**, *124*, 1130.
(9) Li, Y.; Houk, K. N. *J. Am. Chem. Soc.* **1996**, *118*, 880. Deng, Q.; Thomas, B. E.; Houk, K. N.; Dowd, P. *J. Am. Chem. Soc.* **1997**, *119*, 6902.
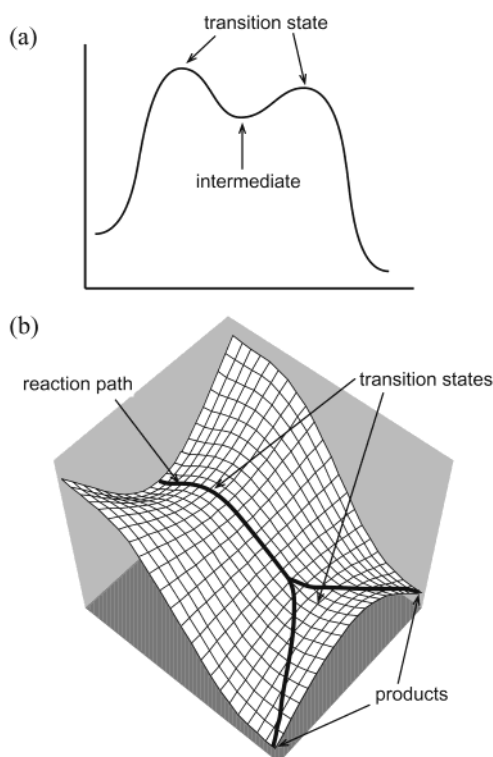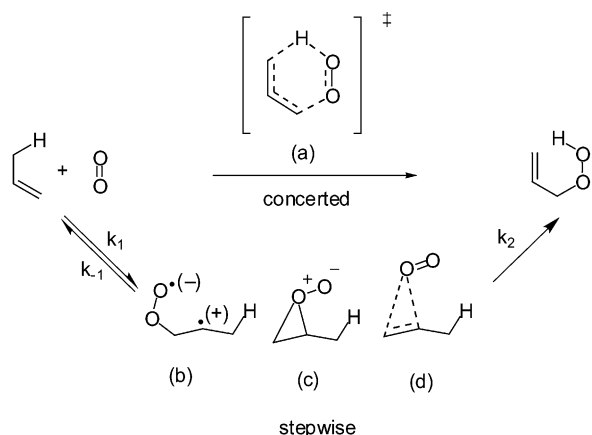
Figure 1. (a) In two dimensions, transition states must be separated by an intermediate. (b) In three dimensions, transition states may be adjacent on an energy surface.

Experimental evidence for the importance of surfaces involving two adjacent transition states has been lacking, and the possibility has been ignored in interpreting experimental observations. We describe here evidence for two sequential transition states in a complex organic reaction, and we discuss how this finding resolves conflicting experimental and theoretical observations in an enigmatic mechanism.
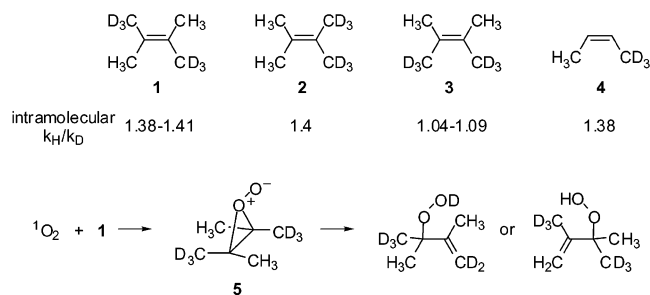
A clear picture of the mechanism of ene reactions of singlet ($^1\Delta_g$) oxygen ($^1O_2$) with alkenes has proved elusive despite extensive experimental and theoretical study. Although the concerted ene reaction (a) is a formally allowed pericyclic process, the absence of significant intermolecular H/D kinetic isotope effects (KIEs) suggests the transition state occurs prior to the product determining step and has focused attention on stepwise mechanisms.[10-12] The question has then become the

identity of the intermediate. Diradical or zwitterionic intermediates (b), perepoxides (c), and π-complexes or exciplexes (d)

have each been suggested. Trapping of intermediates is sometimes observed,[13-15] but not for acyclic alkenes capable of undergoing the ene reaction. The reaction is stereospecifically suprafacial.[16]

The central experimental evidence characterizing the intermediate has come from KIE studies. While the intermolecular isotope effect observed for d_0- versus d_{12}-2,3-dimethyl-2-butene is small (1.11),[11] larger intramolecular isotope effects were observed on the product distribution in the reactions of the stereoisomerically d_6-labeled **1** and **2**.[10,17] However, isomer **3**

exhibited only a small intramolecular isotope effect on the product distribution. Stephenson and Orfanopoulos interpreted these results as strongly implicating an intermediate with the symmetry of a perepoxide.[17] After rate-limiting formation of the perepoxide (and thus no significant intermolecular isotope effect), perepoxides derived from **1** (see **5**) and **2** can select between methyl and deuteriomethyl groups in a product determining step, leading to the observation of an intramolecular isotope effect. A similar intramolecular isotope effect on the product distribution was observed by Foote for the reaction of **4**.[18] The perepoxide derived from **3** would have no such selection available. A diradical intermediate would be expected to exhibit intramolecular isotope effects with **1** and **3** but not **2** or **4**, in contrast to observations.

Unlike experimental studies, theory has usually failed to support the perepoxide. Using a combination of GVB calculations and thermochemical estimates of substituent effects, Harding and Goddard predicted that perepoxide would be 10−16 kcal/mol above the energy of simple starting alkenes + $^1O_2$ and that a diradical intermediate would be preferred by 6−8 kcal/mol.[19] Tonachini and Robb found that initial formation of a diradical was favored in an MC−SCF study of the attack of $^1O_2$ on ethylene.[20] Yamaguchi and Houk had found that
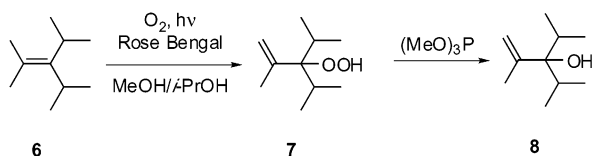
(10) Kopecky, K. R.; van de Sande, J. H. *Can. J. Chem.* **1972**, *50*, 4034.
(11) Gollnick, K.; Hartmann, H.; Paur, H. In *Oxygen And Oxy-Radicals In Chemistry and Biology*; Rodgers, M. A. J., Powers, E. L., Eds.; Academic Press: New York, 1981; pp 379−95.
(12) Stratakis, M.; Orfanopoulos, M.; Foote, C. S. *J. Org. Chem.* **1998**, *63*, 1315.
(13) Jefford, C. W.; Rimbault, C. G. *J. Am. Chem. Soc.* **1978**, *100*, 295. Jefford, C. W.; Rimbault, C. G. *J. Am. Chem. Soc.* **1978**, *100*, 6437. Manring, L. E.; Foote, C. S. *J. Am. Chem. Soc.* **1983**, *105*, 4710. Wilson, S. L.; Schuster, G. B. *J. Org. Chem.* **1986**, *51*, 2056. Fenical, W.; Kearns, D. R.; Radlick, P. *J. Am. Chem. Soc.* **1969**, *91*, 3396.
(14) Frimer, A. A.; Bartlett, P. D.; Boschung, A. F.; Jewett, J. G. *J. Am. Chem. Soc.* **1977**, *99*, 7977.
(15) (a) Poon, T. H. W.; Pringle, K.; Foote, C. S. *J. Am. Chem. Soc.* **1995**, *117*, 7611−7618. (b) Stratakis, M.; Orfanopoulos, M.; Foote, C. S. *J. Am. Chem. Soc.* **1991**, *32*, 863.
(16) Orfanopoulos, M.; Stephenson, L. M. *J. Am. Chem. Soc.* **1980**, *102*, 1417.
(17) Grdina, B.; Orfanopoulos, M.; Stephenson, L. M. *J. Am. Chem. Soc.* **1979**, *101*, 3111.
(18) Orfanopoulos, M.; Smonou, I.; Foote, C. S. *J. Am. Chem. Soc.* **1990**, *112*, 3607−3614.
(19) Harding, L. B.; Goddard, W. A., III *J. Am. Chem. Soc.* **1980**, *102*, 439.
(20) Tonachini, G.; Schlegel, H. B.; Bernardi, F.; Robb, M. A. *J. Am. Chem. Soc.* **1990**, *112*, 483.

unrestricted Hartree−Fock calculations also favor the diradical, though this study also found that the diradical intermediate appeared inconsistent with experimentally observed regioselectivities and stereospecificity.[21] The "cis effect", the preference for hydrogen abstraction from *cis*-substituted groups in trisubstituted alkenes, was interpreted as a consequence of a concerted rather than a stepwise diradical mechanism.[22] These papers and most later theoretical studies have favored a single ene transition state with concerted formation of the C−O and O−H bonds.[23,24] To make this mechanism consistent with the intramolecular isotope effect observations, rate-limiting formation of a π-complex or exciplex with the same symmetry as a perepoxide is a necessary postulate. However, Gorman has argued convincingly on a kinetic basis that exciplex formation cannot be rate limiting.[25]

To summarize, both the diradical and concerted mechanisms have appeared viable theoretically but cannot account for isotope effect observations. The perepoxide, while seeming to provide a clear explanation of the intramolecular isotope effects, has not been a viable intermediate theoretically. These two observations add up to a mechanistic paradox. The combination of experimental and theoretical studies described here suggests a resolution to this paradox involving a reaction surface with two sequential transition states.

Results and Discussion

Intermolecular ^{13}C Isotope Effects. The absence of a significant intermolecular H/D isotope effect in previous studies established that there was no hydrogen abstraction in the rate-limiting step but otherwise provided no information about the structure or symmetry of the rate-limiting transition state. We turned to ^{13}C isotope effects to provide a basic isotope effect characterization of the rate-limiting step. Of particular interest was the symmetry of the rate-limiting transition state; does it involve a symmetrical attack on the olefinic carbons, as might be expected for formation of a perepoxide, or does the ^{1}O$_{2}$ attack at the termini of the π-bond to form a diradical? A difficulty in experimentally probing the transition state symmetry is that symmetrical alkenes inescapably exhibit symmetrical isotope effects because of averaging, while unsymmetrical alkenes necessarily react via unsymmetrical transition states. We therefore chose the "nearly symmetrical" alkene **6** for study. While the olefinic termini of **6** are electronically very similar, differing only in substitution by methyl versus isopropyl groups, the ene reaction of **6** affords the single product **7** from selective hydrogen abstraction from the methyls.

The intermolecular ^{13}C isotope effects for the ^{1}O$_{2}$ ene reaction of **6** were determined combinatorially at natural abundance by

Figure 2. ^{13}C Kinetic isotope effects (k_{12C}/k_{13C}, 10 °C) for the singlet oxygen ene reaction of **6**.

NMR methods.[26] Ene reactions of **6** in 1:1 methanol/2-propanol at 10 °C were taken to 76 ± 2% and 77 ± 2% conversion by irradiation with a sunlamp under a flow of oxygen in the presence of Rose Bengal as sensitizer. Under these conditions, ^{1}H NMR analysis of the crude reaction product exhibited **7** and traces of **8** as the only observable products (see Supporting Information). The reaction mixture was treated with excess trimethyl phosphite at 25 °C to convert **7** to **8**, and the unreacted **6** was then recovered by codistillation with the methanol/2-propanol and partitioning between pentane and water phases to remove the alcohols, followed by fractional distillation. The recovered **6** was then analyzed by ^{13}C NMR compared to a standard sample of **6** from the same synthetic lot that had not been subjected to the reaction conditions. The changes in ^{13}C isotopic composition in **6** were calculated by using the isopropyl methyl carbons as an "internal standard" with the assumption that their isotopic composition does not change. From the changes in isotopic composition, the ^{13}C KIEs were calculated in the previously reported fashion.[26] The results are shown in Figure 2, and there is very good agreement between the two experiments. Similar small isotope effects were observed at each of the olefinic carbons, while the isotope effects at the adjacent methyl and methine carbons were within experimental error of unity.

Qualitatively, these results support an attack of the ^{1}O$_{2}$ on the center of the π-bond, with nearly synchronous bond formation to the olefinic carbons. In principle, the similar olefinic isotope effects could also have resulted from a mixture of two highly unsymmetrical additions to the termini of the π-bond. However, this would require that the rates of attack on the two olefinic carbons be comparable, despite the differing sterics, and each mode of unsymmetrical attack would have to lead to the same product **7**. This seems unlikely. A synchronous attack of ^{1}O$_{2}$ in the rate-limiting transition state would appear to be the most economical explanation for the observed ^{13}C KIEs.

Intramolecular ^{13}C Isotope Effects. Intermolecular KIEs probe only the rate-limiting step and provide no direct information about the rest of a mechanism. The elegant use of *intramolecular* isotope effects to overcome this limitation was pioneered by Dolbier[27] and elaborated by Stephenson and Orfanopoulos.[17] A problem, however, in determining intramolecular isotope effects has been the required regio- or stereospecific synthesis of partially labeled materials. A natural abundance approach to the measurement of intramolecular isotope effects has been recently reported.[28] We describe here the elaboration of this technique to provide a simple ^{13}C analogue of the Stephenson experiment.

(21) (a) Yamaguchi, K.; Yabushita, S.; Fueno, T.; Houk K. N. *J. Am. Chem. Soc.* **1981**, *103*, 5043. (b) Unlike the seemingly similar triazolinedione and nitrosoarene dienophiles, ene reactions with ^{1}O$_{2}$ are notably unselective regiochemically. See: Stratakis, M.; Orfanopoulos, M. *Tetrahedron* **2000**, *56*, 1595.

(22) Houk, K. N.; Williams, J. C.; Mitchell, P. A.; Yamaguchi, K. *J. Am. Chem. Soc.* **1981**, *103*, 949.

(23) Yoshioka, Y.; Yamada, S.; Kawakami, T.; Nishino, M.; Yamaguchi, K.; Saito, I. *Bull. Chem. Soc. Jpn.* **1996**, *69*, 2683.
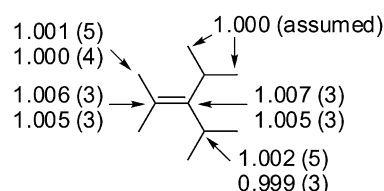
(24) Okajima, T. *Nippon Kagaku Kaishi* **1998**, *2*, 107.

(25) Gorman, A. A.; Hamblett, I.; Lambert, C.; Spencer, B.; Standen, M. C. *J. Am. Chem. Soc.* **1988**, *110*, 8053.

(26) Singleton, D. A.; Thomas, A. A. *J. Am. Chem. Soc.* **1995**, *117*, 9357.

(27) Dai, S.-H.; Dolbier, W. R., Jr. *J. Am. Chem. Soc.* **1972**, *94*, 3946.

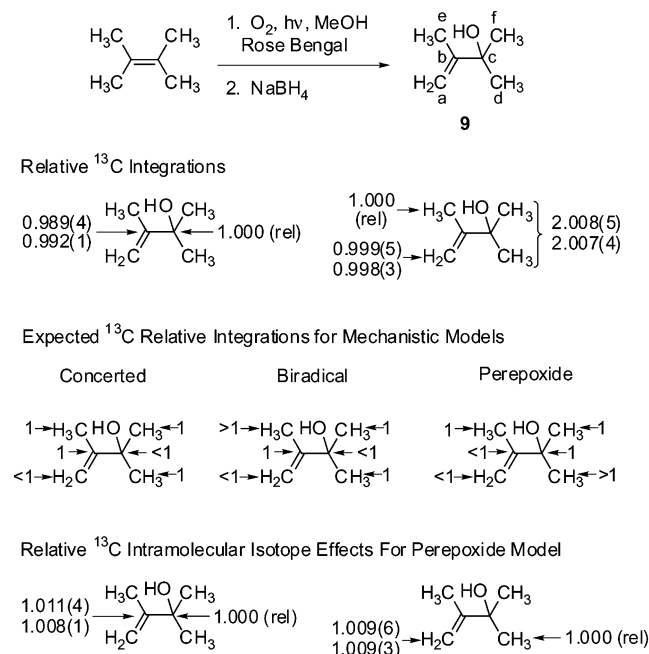(28) Singleton, D. A.; Szymanski, M. J. *J. Am. Chem. Soc.* **1999**, *121*, 9455.

Relative ^{13}C Integrations

Expected ^{13}C Relative Integrations for Mechanistic Models

Concerted   Biradical   Perepoxide

Relative ^{13}C Intramolecular Isotope Effects For Perepoxide Model

Figure 3. Relative ^{13}C integrations for **9**, the pattern of ^{13}C integrations expected for three mechanistic models, and the relative intramolecular ^{13}C KIEs for formation of **9** assuming the perepoxide model.

Using natural abundance tetramethylethylene, 2,3-dimethyl-1-buten-3-ol (**9**) was formed by the ene reaction with $^{1}O_2$ at 0 °C followed by reduction with NaBH$_4$. ^{13}C NMR analysis of **9** was carried out using the recently developed methodology for the accurate and precise measurement of the relative integrations of pairs of peaks within a spectrum.[28] The results are shown in Figure 3. Of the carbons that were originally olefinic in tetramethylethylene, the carbinol carbon (c) of **9** was found to contain a greater abundance of ^{13}C. For the carbons that started as methyl groups in tetramethylethylene, a relatively greater abundance of ^{13}C was found in the geminal methyl groups d and f of **9**.

The interpretation of the integration results is complicated because their translation into KIEs depends on an initial choice of mechanistic model. The approach that must be taken, then, is to *assume* a mechanistic model and then see if the observed ^{13}C integrations are consistent with the model. Three models are considered here: (A) concerted, in which intermolecular and intramolecular selectivity are determined simultaneously; (B) diradical, in which rate-limiting unsymmetrical addition of $^{1}O_2$ to the termini of the π-bond is followed by a selection between the two distal methyl groups in the product-determining step; and (C) perepoxide, in which a rate-limiting symmetrical attack of $^{1}O_2$ is followed by a product-determining selection between methyl groups that started cis in tetramethylethylene. To predict qualitatively the pattern of ^{13}C relative integrations expected for these models, we start by assuming that k_{12C}/k_{13C} would be >1 if a carbon is undergoing loss or gain of a bonded atom in a step but that otherwise k_{12C}/k_{13C} would be unity. When k_{12C}/k_{13C} is >1 at a position, the relative amount of ^{13}C in that position in the product would be decreased to <1. This leads to the predicted pattern of ^{13}C relative integrations for the three model mechanisms shown in Figure 3. It should be noted for these predictions that when a selection occurs between two methyl groups in a product-determining step, the decreased rate of reaction of a ^{13}C at a reacting center will necessarily be

balanced by a relative increase in ^{13}C at a nonreacting carbon. From Figure 3, the experimental pattern of ^{13}C integrations appears inconsistent with the concerted and diradical mechanisms but is as expected for the perepoxide model. This strongly supports the conclusion of Stephenson and Orfanopoulos from intramolecular ^{2}H KIEs that the mechanism involves a species after the rate-limiting step with the symmetry of a perepoxide.

Assuming the perepoxide model allows the actual intramolecular ^{13}C KIEs to be calculated. For the perepoxide model, carbons e and one of the geminal methyl groups (say f) should have identical ^{13}C compositions. Subtracting the integration of carbon e from that for carbons d + f allows calculation of the ratio of ^{13}C in carbons a versus d. From this ratio and the ratio of ^{13}C in carbons b versus c, the relative intramolecular isotope effects for these pairs of carbons can be calculated (Figure 3).

Theoretical Calculations. (A) First Iteration. Reactions of $^{1}O_2$ are intrinsically difficult cases for theoretical study, so our initial efforts were focused on determining what accessible level of theory would provide a reasonably accurate picture of the transition structures and energy surface. Toward that end, the ene reaction of $^{1}O_2$ with tetramethylethylene was studied in RHF, CASSCF, and both restricted and unrestricted Becke3LYP calculations, all employing a 6-31G* basis set.[29] By using tetramethylethylene as the ene component, comparisons of the experimental KIEs with predicted values from differing calculational levels could be used to help gauge the accuracy of the calculated structures. The predicted reaction pathways and energies are summarized in Figure 4.[30] Each calculation makes a significantly different prediction, and it will be seen that none satisfactorily accounts for experimental observations.

In contrast to the concerted mechanism deduced from previous ab initio RHF calculations,[23,24] the exploration of the RHF/6-31G* energy surface for the reaction of tetramethylethylene here predicts a two-step mechanism.[31] In this mechanism, the rate-limiting C_s-symmetric transition structure **10** leads to (by an IRC analysis) the perepoxide **11** at 5.9 kcal/mol below the energy of the starting materials. The perepoxide then abstracts a hydrogen atom in a second transition structure (**12**) to form the ene product.

For CASSCF calculations, an 8 electron/6 orbital active space was used to initially explore the energy surface. Important

(29) Frisch, M. J.; Trucks, G. W.; Schlegel, H. B.; Scuseria, G. E.; Robb, M. A.; Cheeseman, J. R.; Zakrzewski, V. G.; Montgomery, J. A., Jr.; Stratmann, R. E.; Burant, J. C.; Dapprich, S. J.; Millam, M.; Daniels, A. D.; Kudin, K. N.; Strain, M. C.; Farkas, O.; Tomasi, J.; Barone, V.; Cossi, M.; Cammi, R.; Mennucci, B.; Pomelli, C.; Adamo, C.; Clifford, S.; Ochterski, J.; Petersson, G. A.; Ayala, P. Y.; Cui, Q.; Morokuma, K.; Rega, N.; Salvador, P.; Dannenberg, J. J.; Malick, D. K.; Rabuck, A. D.; Raghavachari, K.; Foresman, J. B.; Cioslowski, J.; Ortiz, J. V.; Baboul, A. G.; Stefanov, B. B.; Liu, G.; Liashenko, A.; Piskorz, P.; Komaromi, I.; Gomperts, R.; Martin, R. L.; Fox, D. J.; Keith, T.; Al-Laham, M. A.; Peng, C. Y.; Nanayakkara, A.; Challacombe, M.; Gill, P. M. W.; Johnson, B.; Chen, W.; Wong, M. W.; Andres, J. L.; Gonzalez, C.; Head-Gordon, M.; Replogle, E. S.; Pople, J. A. *Gaussian 98*, revision A.11.2; Gaussian, Inc., Pittsburgh, PA, 2001.

(30) The UB3LYP energies of open-shell singlets were corrected by spin projection. See: Yamaguchi, K.; Jensen, F.; Dorigo, A.; Houk, K. N. *Chem. Phys. Lett.* **1988**, *149*, 537. Yamanaka, S.; Kawakami, T.; Nagao, H.; Yamaguchi, K. *Chem. Phys. Lett.* **1994**, *231*, 25. For a caveat on this procedure, see: Wittbrodt, J. M.; Schlegel, H. B. *J. Chem. Phys.* **1996**, *105*, 6574. All of the open-shell singlet species have $\langle S^2 \rangle$ values of approximately 1. Projection lowered the energies by 1−4 kcal/mol. The projection procedure was necessary for UB3LYP to obtain a reasonable value for the singlet−triplet gap in O_2.

(31) The RHF calculations predict that a very loose π-complex is formed without a barrier on the approach of singlet oxygen to the pi bond of tetramethylethylene. The energy of the π-complex was −1.1 kcal/mol relative to those of the separate alkene and singlet oxygen. After allowance for basis set superposition error and entropy, this "complex" is unlikely to correspond to a free-energy minimum at 25 °C.
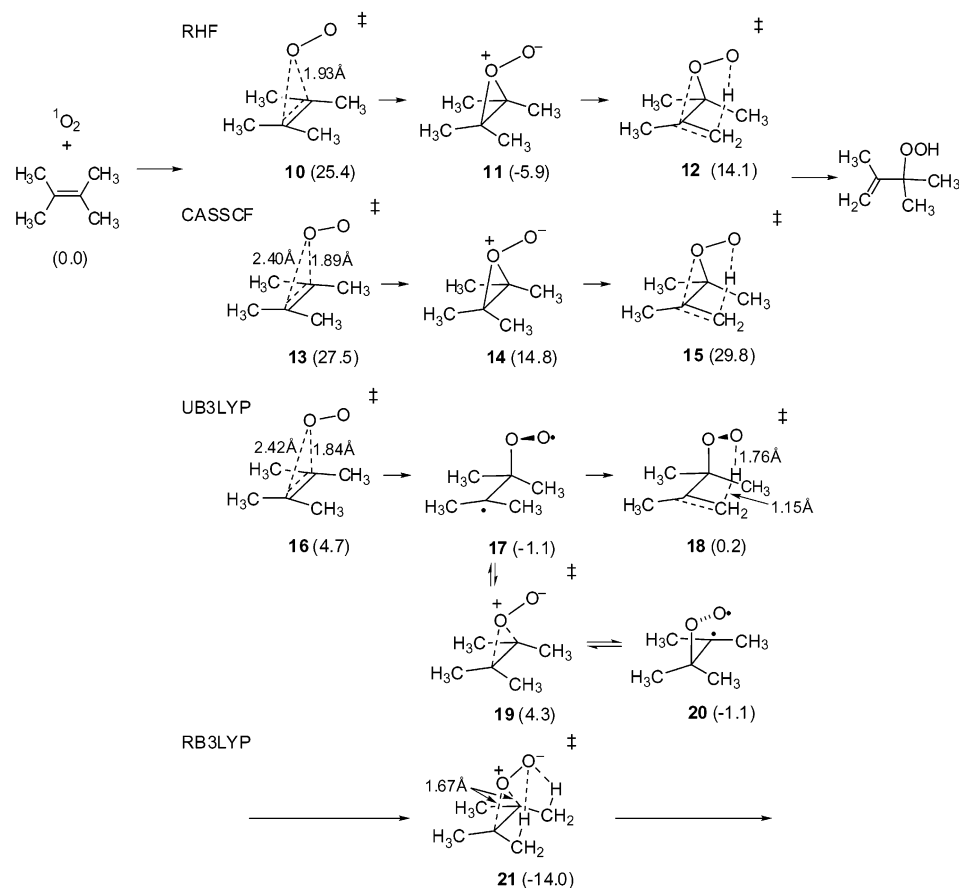
Figure 4. Mechanisms predicted at differing theoretical levels for the reaction of $^1O_2$ with tetramethylethylene. Numbers in parentheses are energies of transition structures relative to the starting materials in kcal/mol, including zpe.

structures were then reoptimized using a 10 electron/8 orbital active space to include σ/σ^* orbitals for C−H. The CASSCF pathway differs from the RHF pathway by involving a nonleast-motion attack of the $^1O_2$ on the alkene. The transition structure **13** is highly unsymmetrical, and there is asynchronous formation of the C−O bonds of the perepoxide **14**. However, the perepoxide **14** and product-forming transition structure **15** are similar to the corresponding RHF structures. The product-forming step is predicted to be rate-limiting at the CASSCF-(10e,8o)/6-31G* level. However, single-point QCISD/6-31G* energies for the CASSCF structures predict the first step to be rate limiting, placing **13**, **14**, and **15** at 2.0, −8.6, and −8.3 kcal/mol, respectively, relative to the starting materials.

The unrestricted Becke3LYP (UB3LYP) pathway also involves a highly unsymmetrical attack of the $^1O_2$, but in this case, the transition structure **16** leads to the formation of the diradical **17**. In the UB3LYP calculation, the perepoxide **19** is a transition structure for interconversion of the regioisomeric diradicals **17** and **20**.[32]

In restricted Becke3LYP (RB3LYP) calculations, there is no potential energy barrier for attack of $^1O_2$ on tetramethylethylene and the only transition structure that could be located on the potential energy surface was the C_s-symmetric perepoxide **21**. This transition structure connects regioisomeric product hydroperoxides. The RB3LYP surface was explored systematically in a grid search by fixing the distance between the olefinic

carbons and the attacking oxygen atom. The resulting energy surface (see Supporting Information) exhibits a C_s-symmetric channel for attack of the oxygen on the olefinic carbons. This channel leads toward the C_s perepoxide, though the reaction path would bifurcate shortly before the perepoxide to form the equivalent unsymmetrical products. A similar energy surface will be discussed in detail in the next section. Attack of the $^1O_2$ on tetramethylethylene would presumably face a free-energy barrier at some relatively large separation of the oxygen from the alkene, though no free-energy maximum was found in a limited exploration of the surface out to a 3.8 Å separation between $^1O_2$ and tetramethylethylene. There is no point in an exhaustive search for the free-energy saddle point, as entropy calculations on the flat surface at large $^1O_2$/alkene separations are questionable.

Inter- and intramolecular KIEs based on structures **10**, **12**, **13**, **15**, and **16** were predicted from the scaled theoretical vibrational frequencies[33] by the method of Bigeleisen and Mayer.[34] Tunneling corrections were applied for steps involving oxygen attack on the alkene using the one-dimensional infinite parabolic barrier model.[35] Because of the questionable accuracy of simplistic tunneling corrections for hydrogen-abstraction steps, no tunneling correction was applied in these cases. A more

(32) Spin-projected UB3LYP/6-311++G** puts **18** 1.2 kcal/mol above the energy of **17** and **19** 5.2 kcal/mol above the energy of **17**, virtually identical to the spin-projected UB3LYP/6-31G* energetics.

(33) For the calculations, the program QUIVER was used (Saunders, M.; Laidig, K. E.; Wolfsberg, M. *J. Am. Chem. Soc.* **1989**, *111*, 8989) with Becke3LYP and RHF frequencies scaled by 0.9614 and 0.91, respectively (Scott, A. P.; Radom, L. *J. Phys. Chem.* **1996**, *100*, 16502).

(34) (a) Bigeleisen, J.; Mayer, M. G. *J. Chem. Phys.* **1947**, *15*, 261. (b) Wolfsberg, M. *Acc. Chem. Res.* **1972**, *5*, 225.

(35) Bell, R. P. *The Tunnel Effect in Chemistry*; Chapman & Hall: London, 1980; pp 60−63.

Table 1. Predicted versus Experimental Intermolecular and Intramolecular Isotope Effects for the Ene Reaction of Singlet Oxygen with Tetramethylethylene

	RHF	CASSCF	UB3LYP no equil[a]	UB3LYP equil[b]	CCSD(T)// B3LYP[c]	experimental
intermolecular						
olefinic ¹³C	1.021	1.039[d]	1.034[d]	1.034[d]	1.007	1.005−1.007[e]
d_0/d_{12}	0.92	0.97	1.10	1.10	1.113	1.11[f]
intramolecular						
olefinic ¹³C	1.026	1.018	0.968	1.016	g	1.011(4), 1.008(1)
reacting methyl ¹³C	1.013	1.015	h	1.011	g	1.009(6), 1.009(3)
²H KIE in **1**	3.13	5.14	1.68	1.69	g	1.38−1.41[i]
²H KIE in **2**	3.40	5.90	1.21	2.11	g	1.4[j]
²H KIE in **3**	1.04	1.29	1.69	1.03	1.045	1.04−1.09[i]

[a] Assuming no equilibration of **17** and **20** and that C−O rotation in **17** allows both distal methyl groups to react. [b] Assuming rapid equilibration of **17** and **20** and that C−O rotation in **17** and **20** is slow. [c] See text for description. [d] On the basis of an average of the predicted olefinic KIEs. [e] On the basis of the KIEs observed for **6**. [f] See ref 11. [g] Not predictable from transition state theory. See ref 45 for a dynamical analysis of the ²H KIEs. [h] The prediction cannot be compared with the experimental KIE listed because the experimental number is based on a conflicting mechanistic assumption. [i] See ref 17. [j] See ref 10.

complete treatment would normally raise the isotope effect, so the calculated KIEs in the absence of tunneling are useful as lower-bound predictions. The results are summarized in Table 1. The absence of an intermediate for the RB3LYP pathway precludes calculation of intramolecular isotope effects by transition state theory.

Qualitatively, the mechanisms predicted by the RHF and CASSCF results lead to predicted KIEs that are largely in the same direction as the experimental observations. Quantitatively, however, the KIE predictions are poor. In contrast to the small observed ¹³C KIEs for the olefinic carbons of **6**, both calculations predict large intermolecular ¹³C KIEs. The pattern of intramolecular KIEs predicted from the RHF and CASSCF pathways fits with the experimental values, but in every case, the predicted KIE is far too large. These results suggest that the calculated geometries for both pathways are at least quantitatively inaccurate.
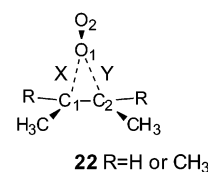
In evaluating the UB3LYP diradical mechanism, we considered two distinct mechanistic possibilities. The first possibility is that the diradical **17** acts in accord with the classical expectations that Stephenson assumed. That is, it is assumed that **17** does not equilibrate with **20** and that in **17** there is an equal chance of hydrogen abstraction at the two distal methyl groups. As shown in Table 1, the predicted isotope effects for this mechanism disagree with experiment in several ways. Most notably, the predicted intramolecular olefinic ¹³C KIE is in the wrong direction and the predicted intramolecular ²H KIEs have the wrong pattern versus experiment. This mechanism is excluded.

The second possibility to consider for the UB3LYP diradical mechanism is that the diradicals **17** and **20** could equilibrate via the perepoxide transition structure **19**. Theoretical and experimental support for a similar equilibration of diradicals has been presented for ene reactions of triazolinediones[36] and nitrosoalkenes.[37] However, the UB3LYP calculations do not predict such a mechanism here; the UB3LYP barrier for

equilibration (5.4 kcal/mol; see Figure 4) is higher than that for product formation (1.3 kcal/mol). The same is true in CCSD-(T)/6-31G* single-point energy calculations, where the **17**/**20** equilibration barrier increases to 8.2 kcal/mol, so the equilibration of diradicals would not be expected. Despite this, the isotope effects for the equilibration mechanism were calculated for comparison with experiment. For this calculation, it was assumed that the equilibration of **17** and **20** is fast but that rotation about the C−O bond in **17** and **20** is slow; these "best-case" assumptions give the equilibrating **17**/**20** the same effective symmetry as that of a perepoxide. This leads to predictions of intramolecular KIEs (Table 1) that qualitatively fit the pattern of the experimental values, with overall better predictions than the other calculations. However, the quantitative disagreement of the calculated KIEs versus experiment is still substantial, and the lack of theoretical support for the equilibration of **17** and **20** makes this mechanism unlikely.

The predicted intermolecular ¹³C KIEs for all of the calculations were very far from the experimental values. Because there is a significant history of accurate ¹³C KIEs predictions for steps not involving hydrogen transfer,[38] this observation is most dissuasive of the ability of the calculations to depict accurately the reaction surface. Our conclusion is that none of these calculations adequately represent the reaction surface.

(B) Second Iteration. The previous observations indicate that an adequate description of the energy surface for these reactions requires theoretical methodology that includes substantial dynamic configuration interaction. Because the required levels of theory are not readily practical for full geometry optimization, we turned to a composite procedure. A 15 × 15 grid of the reaction surface for attack of ¹O₂ on *cis*-2-butene and on tetramethylethylene was formed by fixing the distance of the attacking oxygen from the olefinic carbons, distances C₁−O₁ (*X*) and C₂−O₁ (*Y*) in **22**, at a series of values and then optimizing all other variables in restricted B3LYP/6-31G* calculations. High-level single-point energy calculations were then carried out for each geometry on the grid (after eliminating points that are redundant by symmetry).

22 R=H or CH₃

Composite grid searches of this type are subject to some dangers, and these are considered here briefly before discussing the results. In any high-level single-point energy calculation on a low-level geometry, an intrinsic assumption is that the error in the low-level geometry is systematic, relative to the hypothetical high-level optimized geometry. This process can fail if the low-level and high-level surfaces differ qualitatively. The B3LYP surface overestimates the energy of ¹O₂ but otherwise closely resembles surfaces calculated at higher levels, particularly as the ¹O₂ draws close (*X* or *Y* < 2.3 Å) to the alkene (see Supporting Information). This supports the validity of using the B3LYP grid geometries. Other dangers arise from the limited two-dimensional exploration of a 3N−6 dimension surface.[39] The

(36) Singleton, D. A.; Hang, C. *J. Am. Chem. Soc.* **1999**, *121*, 11885.
(37) Leach, A. G.; Houk, K. N. *Chem. Commun.* **2002**, 1243.
(38) Meyer, M. P.; DelMonte, A. J.; Singleton, D. A. *J. Am. Chem. Soc.* **1999**, *121*, 10865.
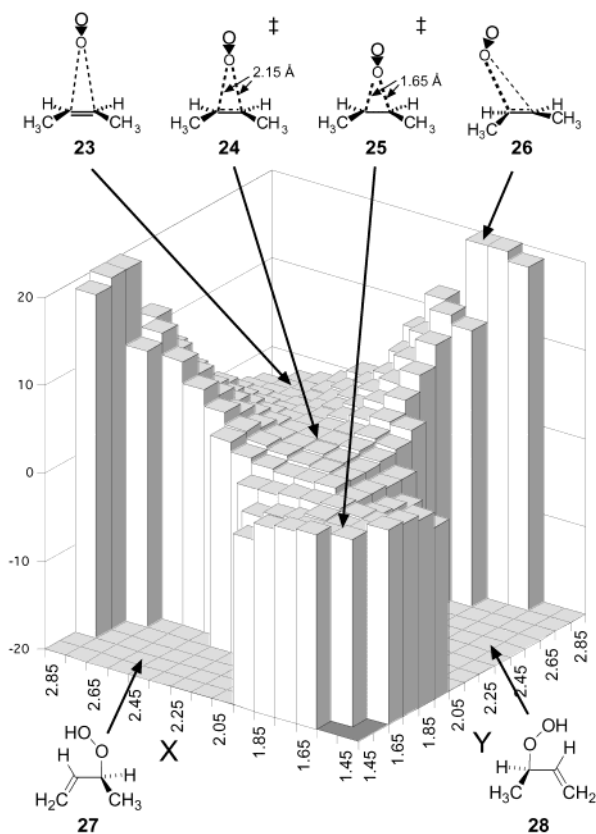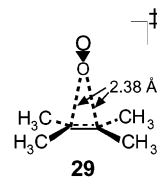
Figure 5. Two-dimensional grid of the CCSD(T)/6-31G*//RB3LYP/6-31G* + zpe energy surface for reaction of $^1O_2$ with *cis*-2-butene. X and Y are C_1-O_1 and C_2-O_1 distances, as defined in **22**. The vertical energy scale is in kcal/mol relative to the energy of the starting materials. The product valleys for **27** and **28** are cut off at -20 kcal/mol but actually extend to -41 kcal/mol.

most critical issue is the question of whether the grid geometries are germane to the reaction path. To address this issue for the B3LYP surface for $^1O_2$/tetramethylethylene, the minimum-energy path (MEP) was followed downhill, in mass-weighted coordinates, starting from a C_s-symmetric structure with $X = Y = 2.85$ Å and proceeding toward **21**. The resulting path proceeded through all of the relevant C_s-symmetric grid geometries. Starting from **21** and proceeding toward products, the MEP involves no significant hydrogen transfer until X or Y increases from 1.67 Å to over 2.0 Å. Nearer to **21** than this, the MEP very closely follows the grid geometries. These observations support the relevance of the grid geometries to the reaction path.

The grid for the $^1O_2$/*cis*-2-butene reaction was examined using several levels of single-point calculations, including MP4(sdtq)/6-31G*, MP4(sdtq)/6-311+G**, and CCSD(T)/6-31G*. All three give very similar results (see Supporting Information). The CCSD(T)/6-31G* results are shown pictorially in Figure 5. The grid for attack of $^1O_2$ on tetramethylethylene was studied only partially at CCSD(T)/6-31G*, and the surface is analogous to the $^1O_2$/*cis*-2-butene surface (see Supporting Information).

The CCSD(T)//B3LYP (+ zpe) surface in Figure 5 predicts a symmetrical attack of the $^1O_2$ through a relatively early transition state **24** [$X = Y = 2.15$ Å for *cis*-2-butene and 2.38 Å for tetramethylethylene (**29**)]. At this first transition state,

hydrogen abstraction has not yet started; in fact, the reaction has not yet "decided" which hydrogen to abstract. From **24**, the reaction path appears to lead toward perepoxide-like structure **25**. However, **25** is not an intermediate! There is no enthalpic or entropic barrier for its decomposition.[40] This "perepoxide" *is a transition state*, formally connecting the two product valleys **27** and **28**. These products are formed from **25** by hydrogen abstraction, but as described above, C—H bond breaking does not become significant until there is substantial desymmetrization of the C_s-symmetric **25**. The minimum energy path connecting reactants with products becomes unstable between rate-limiting transition state **24** and perepoxide transition state **25** at the valley—ridge inflection.[1-5,41] Intermolecular selectivity between alkenes and product selectivity in **3** would be decided in the rate-limiting transition states (**24** or **29**), while product selectivity for reaction among groups that started cis on the alkene would be decided in the area of the valley—ridge inflection.

The use of CCSD(T) calculations here is subject to concern over whether a single-reference electron-correlation procedure is sufficient to represent the reaction surface. We examined this question in two ways. First, the T_1 diagnostic of Lee was calculated for each of the grid points.[42] For this diagnostic, T_1 values > 0.02 suggest that nondynamical correlation effects are large enough to make single-reference methods limited to single and double excitations potentially unreliable. The inclusion of a perturbative correction for triple excitations, as in CCSD(T) here, will satisfactorily compensate for the deficiencies of a single-determinant reference under certain circumstances,[43] but the T_1 value remains a flag indicative of possible danger. The T_1 values (see Supporting Information) are unsurprisingly low (0.012−0.017) in the product valleys, but they are also low (0.013−0.020) as the $^1O_2$ approaches the alkene up to the rate-limiting transition state **24**. However, the T_1 values are increased (0.021−0.031) in the area between **24** and **25** in Figure 5, and T_1 reaches a maximum of 0.036−0.037 at the edge of the "cliff" above the product valley (from $X = 1.55$ Å, $Y = 1.95$ Å to $X = 1.75$ Å, $Y = 2.15$ Å in Figure 5). The second way in which

(39) An obvious but surmountable problem is that any particular values of X and Y do not by themselves *uniquely* define the molecular geometry. It is therefore necessary to describe in detail the process by which the structures were obtained. Starting from a C_s-symmetric structure with $X = Y = 2.85$ Å, we obtained a series of C_s-symmetric structures by decreasing the fixed X and Y by 0.1 Å and reoptimizing the geometry at each step. Series of nonsymmetrical structures were obtained from the C_s-symmetric structures by successively decreasing X by 0.1 Å, leaving Y constant, and reoptimizing the geometry at each step.

(40) As the structure departs from the saddle point along the MEP, a low-energy rotational mode in the nonreacting methyl group is loosened, and overall, the entropy is increasing (on the basis of B3LYP frequencies, 298 K). There is thus no indication of a free-energy barrier to the decomposition of the perepoxide.

(41) Kraus, W. A.; DePristo, A. E. *Theor. Chim. Acta* **1986**, *69*, 309.

(42) (a) Lee, T. J.; Rice, J. E.; Scuseria, G. E.; Schaefer, H. F., III. *Theor. Chim. Acta* **1989**, *75*, 81. (b) Lee, T. J.; Taylow, P. R. *Int. J. Quantum Chem. Symp.* **1989**, *23*, 199.

(43) (a) Kraka, E.; Cremer, D. *J. Am. Chem. Soc.* **1994**, *116*, 4929. (b) Wesolowski, S. S.; Fermann, J. T.; Crawford, T. D.; Schaefer, H. F., III. *J. Chem. Phys.* **1997**, *106*, 7178. (c) Kraka, E.; Cremer, D. *J. Am. Chem. Soc.* **2000**, *122*, 8245. (d) Lindh, R.; Lee, T. J.; Bernhardsson, A.; Persson, B. J.; Karlstrom, G. *J. Am. Chem. Soc.* **1995**, *117*, 7186. (e) Cramer, C. J. *J. Am. Chem. Soc.* **1998**, *120*, 6261.

the multireference character of the wave function was examined was by looking at the stability of the restricted singlet wave function. The wave function was unsurprisingly UHF unstable when the $^1O_2$ is distant from the alkene (the same is true for $^1O_2$ by itself), but the wave function was uniformly both singlet and triplet stable in the areas of the surface where T_1 was high. The two tests are therefore somewhat contradictory.[44] Overall, it is apparent that comparison with experimental observations will be necessary for a decisive validation of the CCSD(T) surface.
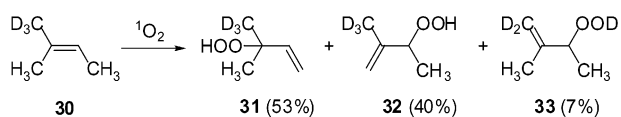
Experimental Support. Unfortunately, selectivity in the area of the valley−ridge inflection of Figure 5 cannot be analyzed using transition state theory. Without a barrier, transition state theory simply does not apply, and a dynamics approach is required. This is the subject of an accompanying paper, which concludes that the intramolecular ^2H KIEs in **1** and **2** are consistent with dynamical selectivity on the type of surface in Figure 5.[45]

Isotope effects allow a careful scrutiny here of the energy surface in the area of the rate-limiting transition state. The intermolecular ^2H and ^{13}C KIEs for the tetramethylethylene reaction as well as the intramolecular ^2H KIE in **3** were predicted from transition state theory using a numerically calculated CCSD(T) frequency along the reaction coordinate and the B3LYP frequencies for all other modes in the rate-limiting grid saddle point **29**. The results are given in Table 1. In contrast to the other theoretical methods examined, the composite CCSD-(T)/6-31G*//B3LYP/6-31G* grid results in excellent KIE predictions. In each case, the calculated KIEs are within error of the experimental values, and the level of agreement is quite striking.

The predicted energy barrier for reaction of $^1O_2$ with tetramethylethylene at the rate-limiting grid saddle point is −2 kcal/mol (CCSD(T)/6-31G*//B3LYP/6-31G* + zpe), and the predicted entropy of activation (B3LYP/6-31G*) is −34 eu. This is in very good agreement with the experimental values −0.74 kcal/mol and −30.1 eu, respectively.[25]
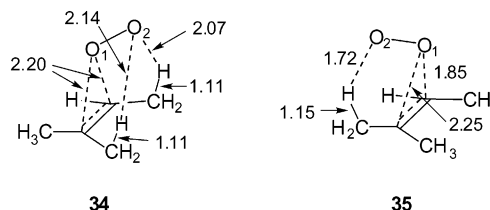
Our conclusion from these results is that **29** is an accurate depiction of the rate-limiting transition state for reaction of $^1O_2$ with tetramethylethylene and that the CCSD(T) grid provides an accurate representation of the energy surface in the area around **29**. This supports the accuracy of the CCSD(T) grid for the rest of the surface.

Cis Effect. With trisubstituted alkenes and enol ethers, there is a notable and general trend for singlet oxygen to abstract allylic hydrogens from the disubstituted side of the alkene.[22,46−49] The simplest example of this "cis effect" is the reaction of **30**, where 93% of the products result from reaction of the initially cis methyl groups. (The isotope effect here is nearly negligible.[47])

30   **31** (53%)   **32** (40%)   **33** (7%)

To investigate the cis effect, a grid search was conducted for the two possible rate-limiting transition structures for attack of $^1O_2$ on 2-methyl-2-butene. This search employed, as earlier, CCSD(T)/6-31G* single-point energies on B3LYP geometries.

The approximate transition structure **34**, leading to reaction of one of the initially cis methyl groups, is a synchronous attack on the olefinic carbons. In **34**, there is a close contact between O2 and hydrogens on the cis methyl groups, but there is no C−H bond breaking yet at this stage. In contrast, approximate transition structure **35**, leading to reaction of the lone trans methyl group, is much later than **34** and involves an asynchronous attack on the olefinic carbons. Structure **35** is predicted to be 2.8 kcal/mol higher in energy than structure **34** (CCSD(T)/6-31G*//B3LYP/6-31G* + zpe), so the calculations correctly predict a substantial cis effect.

34   **35**

Significance. The mechanism supported here for reactions of *cis*-2-butene and tetramethylethylene might be described as *concerted* in normal parlance, in that there is no intermediate between starting materials and product. In this respect, previous theoretical calculations predicting a concerted reaction were correct. However, the inability of previous calculations to explain experimental observations highlights the problem with the use of the word "concerted" as a synonym for "no intermediate". The meaning of the scientific word "concerted" arises from its more catholic meaning of events happening in unison, which is certainly not a satisfactory description here.

Dewar described reactions as "two stage" when the bonding changes in a concerted reaction are unequal at the transition state.[50] The "two-stage" term may apply here, but it is quite an understatement. In this way, the $^1O_2$ ene mechanism is related to a number of thermal hydrocarbon rearrangement reactions, such as 1,3-sigmatropic shifts in vinylcyclopropanes and vinylcyclobutanes.[51−53] In these rearrangement reactions, there is a clear separation between an initial bond-breaking stage and a final bond-making stage. The predicted potential energy surfaces typically exhibit only a single saddle point, but between the stages, there is a nearly flat region corresponding to a diradical "intermediate." In the $^1O_2$ ene mechanism, the separate "stages" are not the result of a flat potential energy surface, but rather, the stages are intrinsically related to the topology of a surface having two adjacent saddle points. For both types of reactions, product distributions will be decided by dynamics effects[54−56] rather than separate barriers for alternative reactions.

We would argue that a distinction should be made in the description of reaction mechanisms when the bonding changes become so disconnected that experimental probes may affect

(44) For a similar example, see: Bach, R. D.; Glukhovtsev, M. N.; Gonzalez, C. *J. Am. Chem. Soc.* **1998**, *120*, 9902.

(45) Singleton, D. A.; Hang, C.; Szymanski, M. J.; Greenwald, E. E. *J. Am. Chem. Soc.* **2003**, *125*, 1176.
(46) Rousseau, G.; LePerche, G.; Conia, P. M. *Tetrahedron Lett.* **1977**, 2517.
(47) Orfanopoulos, M.; Grdina, M. J.; Stephenson, L. M. *J. Am. Chem. So*c. **1979**, *101*, 275.
(48) Schulte-Elte, K. H.; Rautenstrauch, V. *J. Am. Chem. Soc.* **1980**, *102*, 1738.
(49) Prein, M.; Adam, W. *Angew. Chem., Int. Ed. Engl.* **1996**, *35*, 477−94.
(50) Dewar, M. J. S. *J. Am. Chem. Soc.* **1984**, *106*, 209.
(51) Nendel, M.; Sperling, D.; Wiest, O.; Houk, K. N. *J. Org. Chem.* **2000**, *65*, 3259.
(52) Beno, B. R.; Wilsey, S.; Houk, K. N. *J. Am. Chem. Soc.* **1999**, *121*, 4816. Wilsey, S.; Houk, K. N.; Zewail, A. H. *J. Am. Chem. Soc.* **1999**, *121*, 5772.
(53) Leber, P.; Baldwin, J. E. *Acc. Chem. Res.* **2002**, *35*, 279.
(54) Carpenter, B. K. *Angew. Chem., Int. Ed.* **1998**, *37*, 3340.

one of the bonding changes without the other. Despite the lack of an intermediate in the $^1O_2$ ene reaction, the mechanism involves *two kinetically distinguishable steps*. The steps are distinguishable in that the overall rate of the reaction and the product distribution may be influenced separately, that is, through isotopic substitution. This is very unlike most "two-stage" mechanisms, such as an asynchronous Diels−Alder reaction. Kinetically, the ene reaction of $^1O_2$ with simple alkenes behaves in every way like a regular two-step mechanism. We would therefore describe the reaction as involving a "two-step no-intermediate mechanism".

The only directly observable difference between a two-step no-intermediate mechanism and a regular two-step mechanism involving a discrete intermediate occurs if the intermediate is trappable. Early reports of trapping an intermediate in the ene reaction of $^1O_2$ with tetramethylethylene were later discounted.[57] Extensive efforts by one of our groups to trap an intermediate perepoxide have failed with any simple alkene capable of undergoing the ene reaction. Of course, these observations only show that an intermediate, if present, has a very short lifetime. In two-step mechanisms, there is a continuum of possible intermediate lifetimes, down to a few femtoseconds. From this viewpoint, a two-step no-intermediate mechanism is just the extreme of the continuum.

This continuum is illustrated further by the consideration of unsymmetrical alkenes. The shape of the potential surfaces shown in Figures 1 and 5 can occur for the singlet oxygen reaction only when the transition state leads to a valley−ridge inflection that can form two products, such as with tetramethylethylene or *cis*-2-butene. With *trans*-2-butene, isobutylene, propene, or related unsymmetrical alkenes, the valley on one side of the ridge necessarily disappears, and the potential surface becomes closely related to other two-*stage* mechanisms involving one transition state and a plateau that leads to product without a second barrier. The reaction coordinates for the symmetrical and unsymmetrical alkenes may be very similar, but for the unsymmetrical alkenes the second stage would not have experimental consequences.

Conclusion

Qualitatively, the intermolecular and intramolecular ^{13}C isotope effects for reactions of **6** and tetramethylethylene, respectively, support the general picture of the mechanism that had been previously concluded from intramolecular ^2H KIEs, and they provide additional detail. The initial attack of $^1O_2$ on **6** occurs at the center of the π-bond with an early transition state. After the rate-limiting transition state, the mechanism involves a species with the effective symmetry of a perepoxide.

Quantitatively, the isotope effects have allowed us to triage the differing mechanisms predicted by various theoretical methods. All of the geometry-optimizable methods employed lead to poor predictions of the experimental KIEs. It is particularly noteworthy that our best efforts at CASSCF calculations did not afford accurate results. The limitations of these calculations have been previously documented, but the results here suggest caution in the interpretation of recent CASSCF calculations looking at other $^1O_2$ reactions.[58]

The composite use of CCSD(T) single-point energies on a grid of B3LYP geometries lead to an excellent prediction of the experimental intermolecular KIEs and intramolecular KIE with **3**. This strongly supports the accuracy of the composite surface in the area around the rate-limiting transition state and, by extension, supports the accuracy of the rest of the predicted reaction surface. The unique feature of this surface is that it involves two adjacent saddle points with no intervening intermediate. Accompanying dynamics calculations support the consistency of the intramolecular KIEs in **1** and **2** with selectivity around the valley−ridge inflection of this surface.[45] The paradox where experiment supports an intermediate but theory does not is resolved; there is no intermediate, but a two-step no-intermediate mechanism can exhibit product selectivity not related to the rate-limiting transition state.

The results here provide the first experimental support for a reaction surface involving two adjacent transition states. However, from the growing number of theoretically predicted cases, there is no reason to think that surfaces involving adjacent saddle points should be rare. When experimental observations are interpreted, the inadequacy of the two-dimensional picture of Figure 1a should be remembered.

Experimental Section

Ene Reaction of 6. Example Procedure. A stream of O_2 was slowly bubbled through a mixture of 19.71 g (141 mmol) of 2,4-dimethyl-3-isopropyl-2-pentene (**6**),[59] 14.66 g of 1,2-dichloroethane (as GC standard), 2.0 g (2.0 mmol) of Rose Bengal, 210 mL of methanol, and 210 mL of 2-propanol at ∼10 °C while the mixture was being irradiated with a 300-W sunlamp. After 26 h, the reaction was found to be 76 ± 2% complete by GC analysis. The irradiation was stopped, and 23 mL (24.2 g, 195 mmol) of trimethyl phosphite was added dropwise at 5−10 °C. The reaction mixture was stirred overnight at 25 °C, at which time no residual hydroperoxide could be detected by GC. The volatiles were then collected by a crude distillation (**6** appears to form an azeotrope with the alcohols) and partitioned between 200 mL of pentane and 400 mL of water. The aqueous layer was extracted with a second 200-mL portion of pentane. The combined pentane layers were rinsed with four 250-mL portions of water, dried (MgSO$_4$), and passed through a 6-in. pad of silica, rinsing with pentane. The resulting solution was subjected to two successive fractional distillations using 30-cm and 10-cm Vigreaux columns to afford 2.35 g of the unreacted **6** (12%, 50% recovery, bp 148−150 °C).

An analogous reaction using 19.0 g of 2,4-dimethyl-3-isopropyl-2-pentene was taken to 77 ± 2% conversion, and 3.4 g of unreacted alkene was recovered.

Ene Reaction of Tetramethylethylene. Example Procedure. A stream of O_2 was slowly bubbled through a mixture of 20.64 mL (14.61 g, 173.6 mmol) of tetramethylethylene and 112 mg (0.11 mmol) of Rose Bengal in 100 mL of dry methanol at 0 °C while being irradiated with a 300-W sunlamp. After 4 d, the irradiation was discontinued, 7.18 g (190 mmol) of NaBH$_4$ was added, and the mixture was stirred at 25 °C for 2 h. After the addition of 100 mL of water, the mixture was extracted with three 50-mL portions of pentane. The com-

(55) Carpenter, B. K. *J. Am. Chem. Soc.* **1995**, *117*, 6336. Reyes, M. B.; Carpenter, B. K. *J. Am. Chem. Soc.* **2000**, *122*, 10163. Reyes, M. B.; Lobkovsky, E. B.; Carpenter, B. K. *J. Am. Chem. Soc.* **2002**, *124*, 641. Carpenter, B. K. *J. Am. Chem. Soc.* **1996**, *118*, 10329.

(56) Doubleday, C., Jr.; Bolton, K.; Hase, W. L. *J. Am. Chem. Soc.* **1997**, *119*, 5251. Doubleday, C.; Nendel, M.; Houk, K. N.; Thweatt, D.; Page, M. *J. Am. Chem. Soc.* **1999**, *121*, 4720. Doubleday, C. *J. Phys. Chem.* **2001**, *105*, 6333. Doubleday, C., Jr.; Bolton, K.; Hase, W. L. *J. Phys. Chem. A* **1998**, *102*, 3648. Doubleday, C.; Li, G.; Hase, W. L. *Phys. Chem. Chem. Phys.* **2002**, *4*, 304.

(57) Gollnick, K.; Haisch, D.; Schade, G. *J. Am. Chem. Soc.* **1972**, *94*, 1747.

(58) (a) Bobrowski, M.; Liwo, A.; Oldziej, S.; Jeziorek, D.; Ossowski, T. *J. Am. Chem. Soc.* **2000**, *122*, 8112. (b) Maranzana, A.; Ghigo, G.; Tonachini, G. *J. Am. Chem. Soc.* **2000**, *122*, 1414.

(59) Lion, C.; Dubois, J.-E. *Bull. Soc. Chim. Fr.* **1976**, 1875. Newman, M. S.; Arkell, A.; Fukunaga, T. *J. Am. Chem. Soc.* **1960**, *82*, 2498.

bined pentane layers were dried (MgSO$_4$) and fractionally distilled through a 10-cm Vigreaux column to afford 3.49 g (20%) of **9**, bp 112–115 °C, contaminated with ∼2% of 2,3-dimethyl-2-butanol and 0.5% of pentane.

NMR Measurements. All samples were prepared using a constant amount of analyte (1.70 g for samples of **6**, 1.5 g for samples of **9**) in 10-mm NMR tubes filled with CDCl$_3$ to a constant height of 5.0 cm. The ^{13}C spectra were recorded at 100.58 MHz with inverse gated decoupling. A T_1 measurement was performed on each sample to ensure that the relaxation rates did not change from sample to sample. Integrations were determined numerically using a constant integration region for each peak of 10 times the width at half-height. A zeroth order baseline correction was generally applied, but in no case was a first order (tilt) correction applied.

The ^{13}C spectra of **6** were taken at a controlled temperature of 50 °C, using 244-s delays between calibrated 45° pulses, a 11.899-s acquisition time, and collecting 486 656 points. The results from six measurements taken on each of the two samples of recovered **6** and samples of **6** that were not subjected to the reaction conditions are summarized in the Supporting Information.

For the intramolecular isotope effects with **9**, some more special acquisition parameters were used. This included calibrated 90° pulses, a sweep width of 40 000 Hz, a filter bandwidth of 28 000 Hz, and 150-s delays between pulses, collecting 480 000 points and zero-filling to 512 K. The longest T_1 value in **9** was 18.8 s. For comparisons of each relevant pair of peaks, a set of spectra was taken with the transmitter centered between the two peaks. The average results from six measurements on each of two independent samples are shown in Figure 3, with standard deviations shown in parentheses.

Supporting Information Available: Theoretical structures and energies. This material is available free of charge via the Internet at http://pubs.acs.org.

JA027225P